

Multi-Objective Optimized Configuration of Electric Vehicle Fast Charging Station Combined with PV Generation and Energy Storage

Jing Liu

Beijing Institute of Technology
Beijing, China
e-mail: liujingbeijing@foxmail.com

Congzhe Gao*

Beijing Institute of Technology
Beijing, China
e-mail: gcz_fly@163.com

Yecong Cao

Beijing Institute of Technology
Beijing, China
e-mail: chongchong1103@163.com

Abstract—To meet the growing demand for electric vehicle charging, large-scale fast charging stations need to be built. However, due to the randomness and impact characteristics of fast charging load, the construction of electric vehicle charging stations is a huge challenge for current distribution networks with limited power capacitance. Building a fast charging station with a photovoltaic generation system and energy storage system (FCS-PVS&ESS) is a promising solution to this problem. This paper proposes a multi-objective optimization method for the configuration of FCS-PVS&ESS based on dynamic adjustment strategy. Compared with conventional optimization methods, this method considers not only system costs but also power fluctuations and renewable energy shares. Better economic and stable performance was achieved by dynamic adjustment strategy, which changes the ESS upper power limit determined by load characteristics and real-time electricity prices. Non-dominant sort genetic algorithm (NSGA-II) is used to obtain the frontier of Pareto optimal solutions. According to the simulation results, the flexible configuration of PVS and ESS can increase annual income by more than 13%, reduce grid power fluctuation by more than 21%, and the proportion of green renewable energy sources exceeds 6%.

Keywords-fast charging station; load characteristics; dynamic control; multi-objective optimized configuration

I. INTRODUCTION

With the development and utilization of renewable energy worldwide, electric vehicles have played an important role in promoting energy reform and environmental protection. According to China's "New Energy Vehicle Industry Development Plan (2021-2035)", new energy vehicles will account for about 25% of total sales in 2025, and public vehicles will be fully electric vehicles by 2035. Fast charging piles with the power over 100kW can meet basic charging requirements in 10-20 minutes. However, due to the lack of power buffering, the high power and short-term charging load of fast charging stations will exceed the capacity range of the distribution network and seriously affect the stability of the distribution network. [1] [2] [3][4]

The establishment of fast charging stations requires a large-scale expansion of the current distribution network, resulting in huge investments. PVS, as a distributed energy source, can reduce load demand on the distribution network to achieve peak cutting. ESS can store energy during low power consumption periods, and release energy during peak power consumption periods (called load shifting) to improve power utilization. The advantages of building FCS-PVS&ESS are in the following aspects: 1) On-site use of PVS can reduce transmission links and reduce transmission losses. 2) ESS can reduce the power fluctuation caused by PVS and EV charging load. 3) PVS and ESS can provide energy to achieve peak cutting, load shifting, and therefore improve power utilization, reduce the capacity of the distribution network and achieve higher charging station economics [5].

In the related research on the optimal allocation of renewable energy capacity, power supply reliability, pollutant emissions [6] [7], and power supply from the power grid [8] are the optimization goals of capacity allocation but all lack construction cost considerations. The literature [9] considers the peak cutting and load shifting to achieve better grid stability. However, the real-time electricity price difference has not been considered, so it cannot reach the best economic benefits. In the charging and discharging strategy of the energy storage system in literature [10], the authors consider the relationship between battery life and depth of discharge but not considered load characteristics.

This paper analyzes the charging behavior and charging demand of electric vehicles. Taking the urban planning of fast charging stations as an example, based on the traffic flow information of service roads, this paper establishes a daily load model of fast charging stations by the Monte Carlo test. A configuration strategy considering load characteristics and real-time electricity prices is proposed to dynamically adjust the upper limit of the discharge power of ESS. With the lowest daily cost, the minimum variation of power fluctuation, and the largest proportion of new energy supply set as the objectives, the NSGA- II algorithm is adopted to optimize the multi-objective capacity configuration. The structure of this article is as follows. After the introduction, the description and

modeling of each component of FCS-PVS & ESS are described in Section II. Section III is dedicated to the method of optimized configuration for FCS-PVS & ESS. Section IV, simulation results, under the restrictions considered for this study, the performance using dynamic adjustment strategy compared with static strategy, and economic and stability analysis of the results obtained by multi-objective optimized configuration based dynamic adjustment strategy. Finally, the conclusions are drawn in Section V.

II. MATHMATIC MODELING OF FCS-PVS&ESS

A. Photovoltaic Model

The power of PVS is not only related to the light intensity, but also the ambient temperature and meteorological conditions. PVS model is established as following formula [11] [12]:

$$P_{pv}(t) = P_{STC} \frac{G(t)}{G_{STC}} \{1 + k[T_c(t) - T_{STC}]\} \quad (1)$$

$$T_c(t) = T_{EN}(t) + 30 \times \frac{G(t)}{1000} \quad (2)$$

where P_{STC} is the rated output power of a single photovoltaic panel in the standard test environment. $G(t)$ is the light intensity at time t. G_{STC} is the light intensity under the standard test environment, which is 1. K is the power temperature coefficient. $T_c(t)$ is the photovoltaic cell board temperature at time t. T_{STC} is the reference temperature of 25 °C. $T_{EN}(t)$ is the ambient temperature at that time.

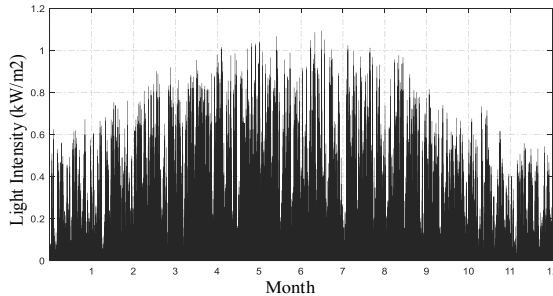


Figure 1. Annual light intensity in Beijing.

Use Homer software to obtain hourly light intensity data throughout the year in Beijing, as shown in Fig. 1. Data are averaged throughout the year to obtain average light values at different times of the day. By selecting ordinary photovoltaic panels and combining with average daily light intensity data, ambient temperature data, and photovoltaic power generation models, the daily photovoltaic power curve of a single photovoltaic panel can be calculated.

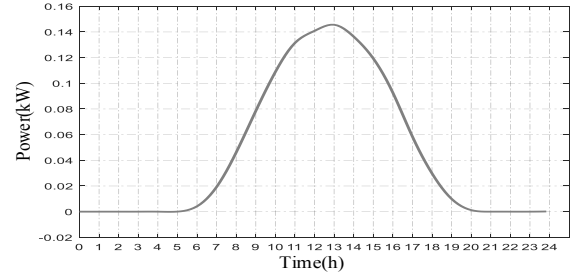


Figure 2. Daily power of a single photovoltaic panel.

B. Load Model

Simulate the charging load of FCS-PVS&ESS. Influencing factors of EV load model are the number of electric vehicles, the battery capacity, and the driving habits of EV owners. To build the load model of urban charging stations, this paper classifies urban passenger cars into four categories according to the purpose -- private passenger cars (private cars), rental passenger cars (rental cars), official passenger cars, and taxis. Official and rental cars have similar driving characteristics, so grouped for the next analysis.

1) The number of electric vehicles

$$n_{ev}(t) = \sum_{n=1}^3 N_{ev}(t) \times D_n \times f_n \times \eta_n \times p_n(t) \quad (3)$$

where $n_{ev}(t)$ refers to the number of vehicles entering the station at time t. $N_{ev}(t)$ refers to the flow of electric vehicles in the service area at time t. D_n refers to the proportion of the different types of vehicles. f_n refers to the frequency entering the charging station in one day. η_n refers to the fast charging choice share. $p_n(t)$ refers to the probability of entering the fast charging station at time t.

TABLE I. FEATURES OF DIFFERENT VEHICLES

Type	Private cars	Rental cars	Taxis
D_n	60%	34%	6%
f_n	0.27	2.0	0.69
η_n	0.0364	1.83	0.28

2) The battery capacity of electric vehicles

Based on the investigation of the current electric vehicle market, cars with 416km of mileage, 51kWh of battery capacity and 12.26kWh of power consumption per 100km is selected as a typical vehicle in the following analysis. It only takes 20 minutes for the model to charge 80% of the electricity in the way of fast charging (120kW / pile).

3) The driving habits of electric vehicles

According to the data of the "2018 China New Energy Vehicle Big Data Research Report", the time-distribution map of three types of passenger cars entering fast charging stations is shown in Fig. 3. It can be seen that three driving styles have

different characteristics. Fig. 4 shows the fitting curves of the time-distribution of three types of habits when terms of entering the charging station.

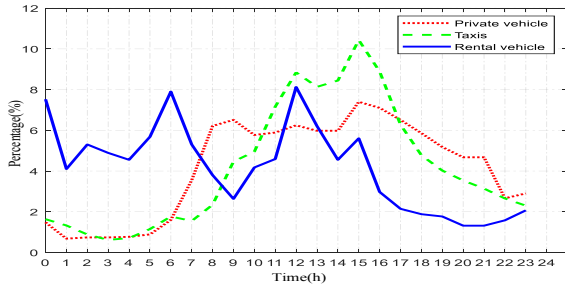


Figure 3. The time distribution of three types of passenger cars entering fast charging stations.

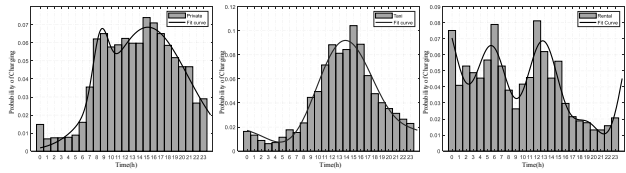


Figure 4. Fitting curves of the time distribution of three types of passenger cars entering the station.

Take the No. 5 fast charging station planned by a certain city in literature [13] as an example. This charging station serves a total of 6 road network nodes, 24 road sections, a service area of 6.72km^2 , and a typical daily traffic volume of 11,505 vehicles. Assuming that the penetration rate of EV is 10%, the number of EV's daily flow is about 1151. Monte

Carlo experiments were performed according to the fitting curve of the probability density distribution function of three types of passenger cars entering the fast charging station to obtain the load demand curve of the power station one day, as shown in Fig. 5.

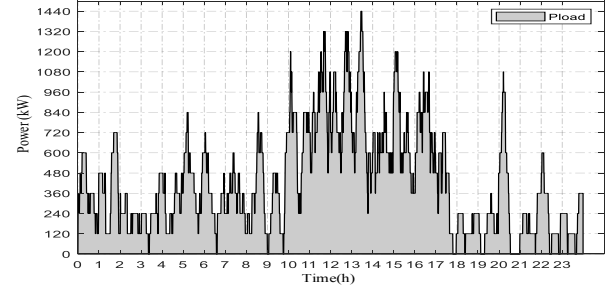


Figure 5. Daily load distribution of charging stations.

As Fig. 6 shown, perform 100 Monte Carlo experiments to get the average daily load demand distribution.



Figure 6. Average daily load distribution of charging stations.

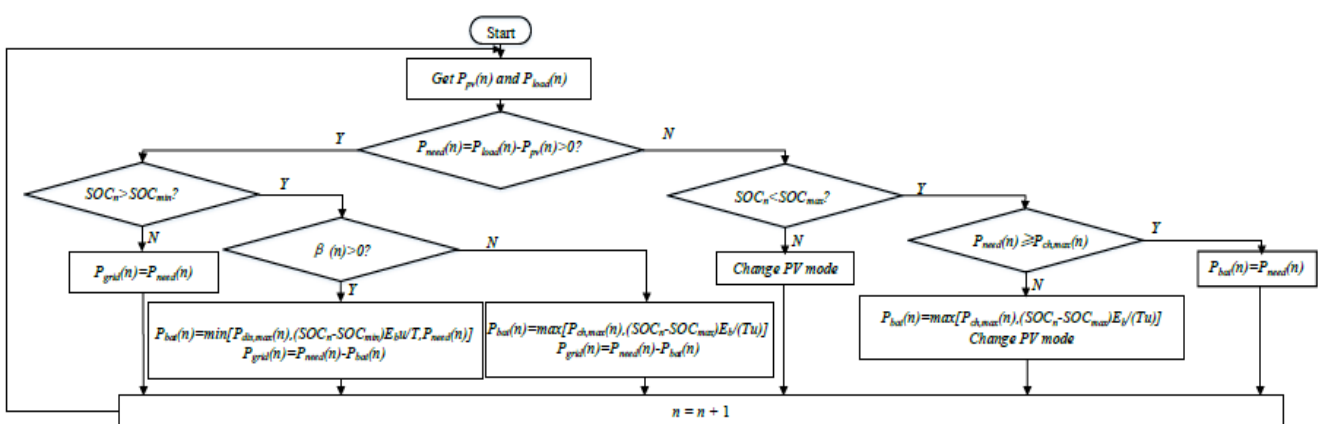


Figure 7. System operation flowchart.

C. Storage System Model

Considering the loss of the battery during charging and discharging, the charging and discharging model of the energy storage system is

$$SOC_t = SOC_{t-1} - P_{bat}T \frac{u}{E_b} \quad (4)$$

$$SOC_t = SOC_{t-1} - \frac{P_{bat}T}{E_b} \quad (5)$$

where SOC_t is the current charging state. SOC_{t-1} is the charging state at the previous moment. T is the interval time.

u is the charge and discharge efficiency. P_{bat} is the real-time power of the storage system, which is positive when discharging and negative when charging. E_b is the capacity of the energy storage system. The first formula is the charging condition, and the second formula is the discharging condition.

III. OPTIMIZED CONFIGURATION METHOD

A. System Operation Strategy

This paper proposes a strategy of setting the upper limit of charging and discharging power in real-time based on load characteristics and real-time electricity price to adjust the operating state of the energy storage system dynamically:

- 1) Obtain the time curve of day load characteristics $P_{load}(n)$;
- 2) Time relationship of obtaining electricity price $C_{grid}(n)$;
- 3) Get the dynamic adjustment coefficient $\alpha(n)$, $\beta(n)$;
- 4) Get the real-time charging and discharging upper limit $P_{ch,max}(n)$ and $P_{dis,max}(n)$.

$$\left\{ \begin{array}{l} P_{pv}(n) = N_{pv} \times P_{pv,each}(n) \\ P_{need}(n) = P_{load}(n) - P_{pv}(n) \\ \alpha(n) = \frac{|C_{grid}(n) \times P_{need}(n) - \overline{C_{grid} \times P_{need}}|}{|\max(C_{grid} \times P_{need}) - \overline{C_{grid} \times P_{need}}|} \\ \beta(n) = \begin{cases} 1 & \text{if } (C_{grid}(n) \times P_{need}(n) - \overline{C_{grid} \times P_{load}}) \geq 0 \\ -1 & \text{if } (C_{grid}(n) \times P_{need}(n) - \overline{C_{grid} \times P_{load}}) < 0 \end{cases} \\ P_{ch,max}(n) = \alpha(n) \times P_{ch,max} \\ P_{dis,max}(n) = \beta(n) \times P_{dis,max} \end{array} \right. \quad (6)$$

The system operation flowchart is shown in Fig. 7. Using $a(n)$ to adjust upper limit of ESS dynamically.

B. Objective Function

1) Lowest average daily investment cost

$$f_i = \min(C - I) \quad (8)$$

where C represents the daily cost of the charging station, and I represents the daily income of the charging station.

$$\left\{ \begin{array}{l} C = (C_1 + C_2 + C_3) / 365 + C_4 \\ C_1 = (C_{CS} + C_{pv} + C_{pile}) \times \frac{r(1+r)^m}{(1+r)^m - 1} \\ C_2 = (C_e \times N_{bat} \times E_{eachBat} + C_p \times P_b) \times \frac{r(1+r)^{m_2}}{(1+r)^{m_2} - 1} \\ C_3 = k_{CS} C_{CS} + k_{pv} C_{pv} + k_{pile} C_{pile} + k_{bat} (C_e E_b + C_p P_b) \\ C_4 = \sum (P_{grid}(t) \times C_g(t)) \\ I = \sum (P_{load}(t) \times (C_g(t) + C_{ser}(t))) \end{array} \right. \quad (9)$$

where C_1 represents the initial construction cost of the charging station. C_2 represents the construction cost of the energy storage system. C_3 represents the operation and

maintenance cost of the charging station. C_4 represents the cost of purchasing electricity from the grid by the charging station.

C_{CS} , C_{pv} , C_e , C_p represent the construction cost of unit capacity distribution station, photovoltaic power generation system, energy storage system, and power conversion device. C_{pile} represents the price of a single charging pile. k_{CS} , k_{pv} , k_{pile} , and k_{bat} represent the maintenance factors of distribution stations, photovoltaics, charging piles, and energy storage systems, respectively.

r is the discount rate. m and m_2 indicate the service life of the charging station and energy storage system.

$E_{eachBat}$ represents the energy of a single battery. P_b represents the maximum discharge power of the energy storage system.

$P_{grid}(t)$ means real-time grid output. $C_g(t)$ means real-time electricity price. $C_{ser}(t)$ refers to the electric vehicle charging service fee.

2) Lowest grid power fluctuation

$$f_2 = \min \sqrt{\frac{1}{N} \sum_{n=1}^N (P_{grid}(n) - \overline{P_{grid}})^2} \quad (10)$$

3) Strongest self-balancing coordination ability

$$f_3 = \min \frac{\sum_{n=1}^N P_{grid}(n)}{\sum_{n=1}^N P_{load}(n)} \quad (11)$$

C. Restrictions

1) Power balance

$$P_{grid}(t) + P_B(t) + P_{pv}(t) + P_{load}(t) = 0 \quad (12)$$

2) Limitation of energy storage system

$$P_{bat}(n) \leq \min[P_{dis,max}(n), (SOC_n - SOC_{min}) \frac{E_b u}{T}] \quad (13)$$

$$P_{bat}(n) \geq \max[P_{ch,max}(n), (SOC_n - SOC_{max}) \frac{E_b}{Tu}] \quad (14)$$

$$SOC_{B,min} \leq SOC_B(n) \leq SOC_{B,max} \quad (15)$$

3) Site constraints

$$\begin{aligned} 0 < N_{PV} &\leq N_{PV,max} \\ 0 &\leq N_B \leq N_{B,max} \end{aligned} \quad (16)$$

$N_{PV,max}$, $N_{B,max}$ represent the maximum number of photovoltaic panels and energy storage batteries.

D. NSGA-II Multi-objective Optimization Algorithm

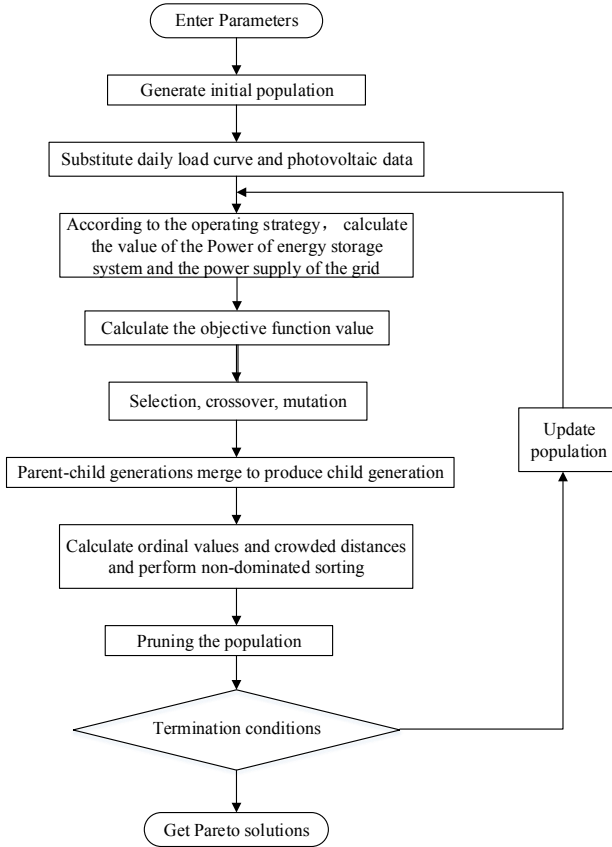


Figure 8. Flowchart of solving optimization model based on NSGA-II.

NSGA-II is one of the most popular multi-objective optimization algorithms with three special characteristics--fast non-dominated sorting approach, fast crowded distance estimation procedure, and simple crowded comparison operator. Through the NSGA-II optimization algorithm, a set of Pareto solutions of this system are finally searched. The optimization process based on NSGA-II is shown in Fig. 8.

IV. SIMULATION RESULTS

A. Research Objects and Basic Data

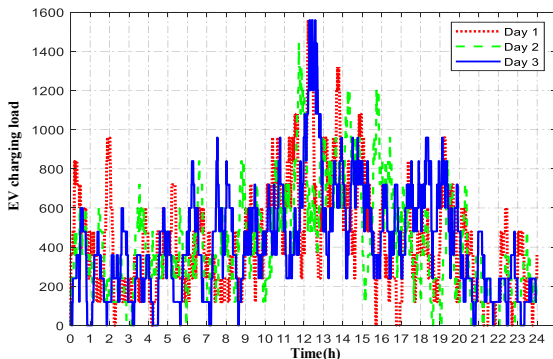


Figure 9. Three-day Monte Carlo load test curve.

According to the load model established in II, a 3-day Monte Carlo test was carried out. The results obtained are shown in Fig.9. Analysis of the daily load power curve shows that the maximum load is 1560kW, the average load is 432.3kW, daily load rate is 27%. The peak period is 11: 00-16: 00. The daily load rate is low, and the time when the load exceeds 800kW is only about 10.65%. Peak maintenance time is short. Therefore, adding photovoltaic power generation units and energy storage systems may have better performance.

Based on the previous average load model, a model of PV-based fast charging station with a storage energy system was established. According to the daily average load curve, eight DC 120kW charging piles are planned to establish in this fast charging station. According to the one-year average light intensity and temperature data of Beijing, the photovoltaic generation model was established. The average daily load power and electricity price curve of Beijing is shown in Fig. 10, with 15min as a node:

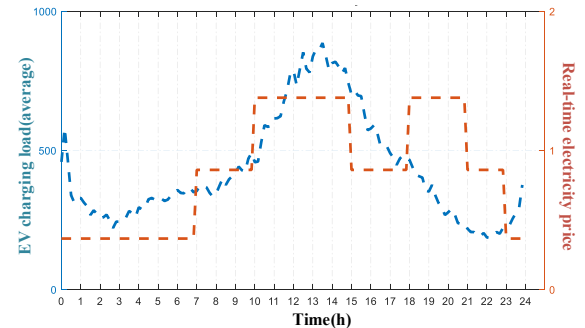


Figure 10. Average daily load and real-time electricity price of Beijing.

B. Dynamic Adjustment Strategy

Compared with the fast charging station without using dynamic adjustment strategy, the results are as follows.

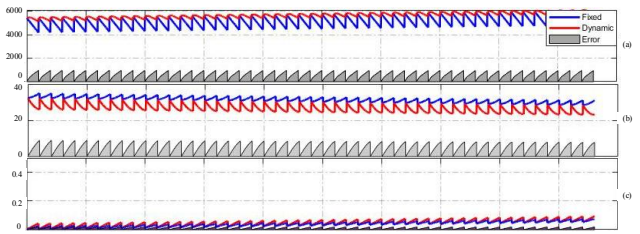


Figure 11. Test results of 9600 configuration schemes. a) is a daily profit under different strategies. b) is a standard deviation of grid power fluctuations under different strategies. c) is a renewable energy share under different strategies.

9600 experiments with varying schemes of configuration were performed to compare the objective function values. The daily benefit of the charging station under dynamic adjustment strategy is higher than that without dynamic adjustment strategy. Grid power fluctuation of the charging station under dynamic adjustment strategy is smaller than that without dynamic strategy. Renewable energy share under dynamic adjustment strategy has little obvious difference

between the two strategies. This is because renewable energy share of the new energy amount is mainly related to the sum of the configured capacity, little influenced by the control strategy of the energy storage system. From the above analysis, the strategy which dynamically adjusts the power limit of ESS achieves better economic performance and system stability.

C. Analysis of Optimization Results

Assume that the site is constrained at 900m², and the maximum energy storage capacity is 1MWh. Under the site constraints, the fast charging station equipped with eight charging piles will be constructed.

1) Capacity configuration sampling experiment

A large-scale configuration sampling experiment is performed, and the objective function is calculated, as shown in Fig. 12.

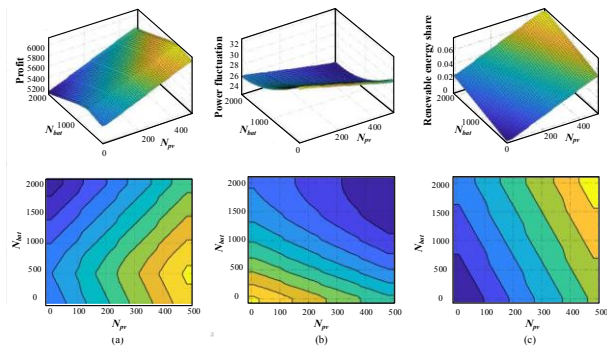


Figure 12. Results of configuration sampling experiment. a) is daily profit under different configurations. b) is standard deviation of grid power fluctuations under different configurations. c) is renewable energy share under different configurations.

It can be seen from Fig. 12:

- the profitability increases with the increase of the number of solar panels, and the deployment of a certain capacity of the storage system with the same capacity of solar energy will increase the profitability;
- grid power fluctuation decreases with the increase of the number of photovoltaic panels and batteries;
- renewable energy share increases as the number of photovoltaic panels and batteries increase;
- when the photovoltaic power output is between 130 ~ 137.5kW, the energy storage capacity is between 250 ~ 300kWh, can achieve the best daily profit.
- when the photovoltaic power is between 115 ~ 137.5kW, the grid stability and new energy output are the best when the energy storage is 1MW.

2) Analysis of NSGA-II algorithm optimization results

Set the optimal front-end individual coefficient Pareto Fraction to 0.35. Set the population size to 200. Set the maximum evolution number Generations to 200. Set the stall generation limit to 200. Set the fitness function deviation value to 1e-6. Use the NAGA-II optimization algorithm to find the Pareto solution distribution as follows.

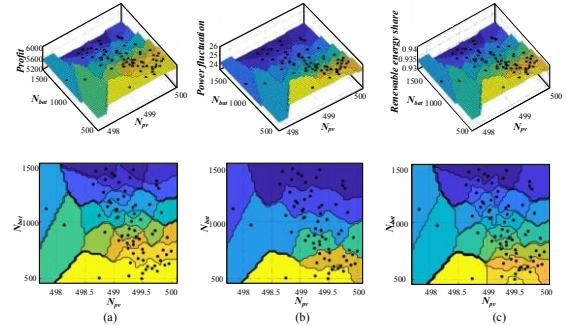


Figure 13. Results of configuration optimization experiment. a) is daily profit under different configurations. b) is standard deviation of grid power fluctuations under different configurations. c) is renewable energy share under different configurations.

Compare the optimization results with the results of sampling experiments, and the Pareto solution set does appear in regions with better performance, which proves that the optimal configuration model can achieve multi-objective optimal configuration. Choose 4 configuration schemes to compare their objective function values.

TABLE II. ANALYSIS OF CONFIGURATION RESULTS

PV (kW)	Storage system (kW·h)	Annual profit (RMB)	Grid power fluctuation (Standard deviation)	Renewable energy share
150	280	↑14.58%	↓21.05%	25.5
150	300	↑14.49%	↓21.36%	25.4
150	400	↑13.96%	↓23.22%	24.8
150	500	↑13.21%	↓25.07%	24.2
0	0	--	1977773	32.3
				0

Compare the Pareto solution obtained from the optimized configuration model with the charging stations without photovoltaic and energy storage systems. The results show that the reasonable configuration of photovoltaic power generation units and energy storage units can achieve better performance in economics, stability, and environmental protection.

TABLE III. RELATED PARAMETERS

Symbol	Value	Symbol	Value
C_{CS}	10220/V·A	k_{pile} ,	0.01
C_{pv}	6000/kWh	k_{bat}	0.01
C_{pile}	62800/pile	r	0.06
C_e	1650/kWh	m	20
C_p	400/kW	m_2	7
k_{CS}	0.01	$E_{eachBat}$	0.576kWh
k_{pv} ,	0.01	$P_{eachPanel}$	0.275kW

V. CONCLUSION

In this paper, the FCS-PVS&ESS model is established based on data. The average daily load-time distribution model of the charging station is established based on 100 Monte Carlo experiments. Based on the real-time electricity price difference and load characteristics, an optimized configuration method using the dynamic adjustment strategy to maximize daily profit, minimize grid power fluctuations, and maximize the proportion of new energy applies. The results of the simulation experiments reached the following conclusions:

1) The dynamic adjustment strategy that dynamically adjusts the upper limit of power of ESS can achieve better benefits and grid output stability.

2) Under the constraints of the site, the results of the equally spaced sampling experiment show that when the photovoltaic capacity is configured between 130 and 137.5 kW, the energy storage capacity is configured between 250 ~ 300kWh to achieve the best daily profit. When the photovoltaic is configured between 115 ~ 137.5kW and the energy storage system is set at 1MW, the grid stability and new energy output are the best;

3) NSGA-II algorithm is used to optimize the configuration. Four groups of optimized configuration results are taken and compared with the performance of the charging station without photovoltaic and energy storage system. The results show that reasonable configuration of PVS and ESS can increase annual income by more than 13%, reduce load fluctuations by more than 21%, and the proportion of green renewable energy sources exceeds 6%.

REFERENCES

- [1] ZHOU Niancheng, PU Songlin, WANG Qianggang, JIANG Guangxue, ZENG Xianping, XIAO Song, CHEN Min, and XIE Jie, "Control strategy of energy storage buffer system for fast charging electric vehicle station," Power System Protection and Control, vol. 41(17), pp.127-134, 2013.
- [2] ZHAO Junhua, WEN Fushuan, YANG Aimin, XIN Jianbo, "Impacts of electric vehicles on power systems as well as the associated dispatching and control problem," Automation of Electric Power Systems, vol. 35(14), pp. 2-10, 29, 2011.
- [3] HU Zechun, SONG Yonghua, XU Zhiwei, LUO Zhuowei, ZHAN Kaiqiao, "Impacts and utilization of electric vehicles integration into power systems," Proceedings of the CSEE, vol. 32(04), pp. 1-10+25, 2012.
- [4] Padej Pao-la-or, Banyat Boribun, "Modeling and Analysis of the Plug-in Electric Vehicles Charging in the Unbalanced Radial Distribution," International Journal of Electrical and Electronic Engineering & Telecommunications, vol. 8(3), pp.133-138, 2019.
- [5] Asatilla Abdulkhakimov, Sanjay Bhardwaj, Gaspard Gashema, and Dong-Seong Kim, "Reliability Analysis in Smart Grid Networks Considering Distributed Energy Resources and Storage Devices," International Journal of Electrical and Electronic Engineering & Telecommunications, vol. 8(5), pp. 233-237, 2019.
- [6] Rodolfo Dufo-López, José L. Bernal-Agustín, José M. Yusta-Loyo, José A. Domínguez-Navarro, Ignacio J. Ramírez-Rosado, Juan Lujano, Ismael Aso, "Multi-objective optimization minimizing cost and life cycle emissions of stand-alone PV-wind-diesel systems with batteries storage", Applied Energy, vol. 88(11), pp.4033-4041, November 2011.
- [7] DUFO-Lopez R, Bernal-Agustin J L, "Multi-objective design of PV-wind-diesel-hydrogen-battery systems", Renewable Energy, vol. 33(12), pp. 2559-2572, December 2008.
- [8] F. J. Ardakani, G. Riahy and M. Abedi, "Optimal sizing of a grid-connected hybrid system for north-west of Iran-case study," 2010 9th International Conference on Environment and Electrical Engineering, Prague, pp. 29-32, 2010.
- [9] HE Yang, ZHANG Yu, WANG Yufei, JIN Shanghe, "Energy Storage Capacity Configuration of PV-integrated EV Charging Station Considering Load Optimization," Modern Electric Power, vol. 36(5), pp. 76-81, 2019.
- [10] LI Wenchao, TONG Yibin, ZHANG Weige, "Energy storage capacity allocation method of electric vehicle charging station considering battery life," Advanced Technology of Electrical Engineering and Energy, vol. 38(4), pp. 55-63, 2019.
- [11] LI Dengfeng, Research on the model and algorithm of power capacity optimization of grid connected microgrid. Chongqing University, 2013.
- [12] ZHANG Yanjie, Analysis and optimization of key factors in economic operation of distributed generation system. Beijing Jiaotong University, 2013.
- [13] FENG Liang, Research on the planning of electric vehicle charging station. Tianjin University,2013.